Anatomic Study: Model Reconstruction from Serial Microscopic Sections

Roman Ďurikovič* and Kazufumi Kaneda

Electric Machinery Laboratory, Faculty of Engineering
Hiroshima University, Japan

Abstract. This paper considers a system for segmenting noisy intensity images and the consequent 3D object reconstruction from a set of planar contours. We propose a new semi-automatic method based on an *active contour model* for extraction of contours from the image. The problem of the topological reconstruction of planar contours is also addressed. The triangulation method must be used to generate the surface enveloping the contours. In this paper we particularly consider the single gap branches and propose the method for their optimal triangulation. The proposed system was successfully applied to the contour extraction and reconstruction processes of a sequence of 636 microscopic images ($7\mu m$ in thickness). The implemented human-computer interaction helps with problems of feature identification and object manipulation about an arbitrary axis.
Key Words: Active shape models, interpolation between polygons, three-dimensional modeling, medical reconstruction

1 Introduction

Reconstruction of a three-dimensional surface or volume model from two-dimensional information is an indispensable technique for better understanding the shape and the position of an organ inside a body.

Although three-dimensional reconstruction is widely used in computer tomography (CT) or magnetic resonance imaging (MRI), the methods do not fulfill all the needs in in the field of anatomy. Anatomists seek information about the exact, overall shape and try to ascertain the features that build it, while in CT, for example, the local abnormalities of known structures are mainly observed. For this reason, a manual sectioning followed by serial microscopy scanning is used. Consequently, an image registration method is greatly needed in anatomical fields that implement serial microscopy.

A set of planar contours extracted from serial sections does not define the required surface itself. First, the contours must be assigned to each other in order to form the object topology, a step called *topological reconstruction*. When the topology is reconstructed, the surfaces interpolated from planar contours have to be generated using a robust triangulation method. The following are the proposed ideas in this paper:

1. An image registration technique based on a mixture of landmark ideas and color combinations is proposed.

*On leave from Department of Computer Graphics and Image Processing, Faculty of Mathematics and Physics, Comenius University, Mlynská dolina, 820 13 Bratislava, Slovakia.

2. A semi-automatic method is proposed in our paper [Ďurikovič et al., 1995] for extracting contours based on the *active contour model* (ACM) [Kass et al., 1987]. The problem of the *potential field* on which the active contour can smoothly slide is considered employing the *feature vector*, based on textural representation of an image space. This approach is an extension of the classical ACM for color image segmentation. Furthermore, our ACM can *change its topology* by fulfilling the heuristic rule of contour division.

3. The topology of the structure is automatically reconstructed, as much as possible, regarding the information about the nesting of contours. The topology of holes can also be reconstructed successfully. Our system also has a topology editor to assist in the correction of the topology.

4. The generation of the triangular patches between consecutive sections using several locally optimal methods, and select the most optimal solution among them is proposed.

Examples of transparent visualization of a mouse embryo and many inner structures support our results.

2 Data Achievement

Using a manual routine processing, a mouse embryo (4.45 mm height) obtained from a "mother mouse" was sectioned with an ultramicrotome, at an average thickness of 7μm sections. Finally, 636 cross-sections which are further processed and stained with hematoxylin-eosin, are obtained. Each cross-section is mounted on glass and then scanned at a magnification of 74 by an optical microscope, to which is attached a photo camera. Images taken from the photo camera are stored in high-resolution compact discs after conversion into digital form. The resolution of digital images was selected to be 720×580.

2.1 Image Registration

Sections from serial microscopy are not only translated or rotated. Often they are deformed due to the heating required in the preparation of the tissue for microscope slices. Thus, serial microscopy requires a combination of a linear transformation to bring the sections into approximate alignment, followed by a nonlinear transformation to account for distortions in the tissue preparation process.

In [Brown, 1992] landmarks are used but it is difficult to see if the results are sufficient or not. In [Carlbon et al., 1994] color combination is used, but without landmarks. The two methods were therefore combined in order to use reference knowledge about image structures (landmarks) and to conform quickly whether the results are acceptable.

First, one landmark is selected on each image. Second, vectors pointed out from the landmarks are selected, as shown in Fig. 1. Vectors and landmarks determine the translation and rotation of images such that the vectors align. Figs. 1a and b show two consecutive sections from a mouse embryo before registration. Figs. 1c shows both sections during the application of the proposed combination of landmark and color merging method. Color differences show how to move the landmarks and rotate vectors to get a better registration.

3 Contour Extraction: the ACM Model

Very good survey about flexible models and their application in model-based vision can be found in [Cootes et al., 1995]. Authors of this paper describe a method for building models by learning patterns of variability from a training set. However, this

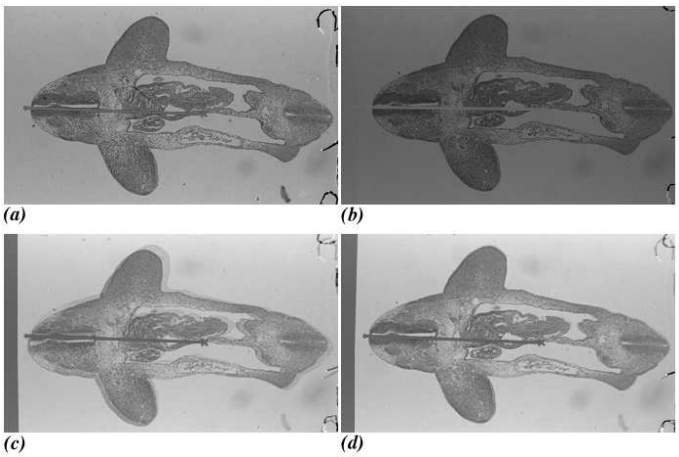

Fig. 1. Image registration of two cross-sections of a mouse embryo. (a) Static image with vector and landmark colored green. (b) Consecutive image with vector and landmark colored magenta. (c) Color merging of transformed and static image. The regions that overlap are some shade of gray. (d) The best registration obtained.

method is applicable for the problem of locating known objects in images. This is not the case in anatomic study, where the shape is often unknown. We found the *active contour model* (ACM) very suitable for 3-D reconstruction in optical microscopy, because it is capable of fitting to very complicated shapes in images.

An ACM is a deformable curve composed of abstract elastic materials minimizing its potential energy. Consider an ACM $v(s,t) = (x(s,t), y(s,t))$ with a spatial parameter s and time t defined on spaces Ω and T, respectively. Let $I(x,y)$ denote the image intensity at position (x,y). The potential energy function of the ACM is defined in [Kass et al., 1987]. In addition, the new energy terms $E_{texture}$ and E_{area} are introduced in the system to extract organs with a particular texture and highly concave shapes, respectively [Ďurikovič et al., 1995]. Each small area of tissue is described with *texture feature vector* $F = (f_1, \ldots, f_7)$, where all vector elements are parameters estimated from the second-order simultaneous autoregressive model [Kashyap and Chellappa, 1987]. The areas where texture features vary dramatically indicate the edges between various tissues. A normalized Euclidean distance measure $\mu(.,.)$ is used as a measure of similarity of two feature vectors. The potential function $E_{texture}$ is then expressed as the distance measure between texture feature vectors F_n^+, F_v, corresponding to both the auxiliary point V_n^+ and the contour point $v(s)$:

$$E_{texture} = \mu(F_n^+, F_v).$$

If $\xi > 0$ is a small constant and N_s is an outer normal vector at contour point $v(s)$, an auxiliary point is given by:

$$V_n^+(s) = v(s) + \xi N_s.$$

Let us note the area delimited by the contour as

$$\int_\Omega E_{area}(v) ds.$$

The total energy is then written as

$$E_{snake} = \frac{1}{2} \int_\Omega \left\{ E_{int}(v) + W_I E_{image}(v) + W_T E_{texture}(v) + W_A E_{area}(v) \right\} ds.$$

The weight functions W_I, W_T and W_A control the *image*, *texture* and *area* energy, respectively.

3.1 Contour Operations

The most fundamental contour operations of adding and deleting a single point are introduced. If the distance between two neighboring points is less/greater than a given threshold, a single point from/between them is deleted/added. For the entire contour, the operation of a contour division into n parts [Ďurikovič et al., 1995] is proposed.

4 Topological Reconstruction

The problem of topological reconstruction is particularly difficult if there are several contours on each plane, and if it is known that the corresponding sub-object can have branches. Geometrical information is employed in topological reconstruction to solve the problem.

Next, the topological reconstruction of two cross-sections is considered. We have three types of connections: a connection between two contours (a so called *cylindrical* connection), a connection between more than two sub-object surfaces forming an *open branch*, and a connection between the sub-object surfaces forming a hole (a *connected branch*).

The automatic topological reconstruction can be summarized in two essential steps. First, the correct contour correspondences must obey the topological position of contours on the slice. This is best described with a *tree of nesting* described in [Shinagawa et al., 1991]. Second, pairs of contours, each one from different cross-sections, are assigned to each other if they satisfy the connectivity criterion having the same level in the nesting tree. Possible branches that appear in the second step are examined further concerning the criteria for open branches. The connected branches (holes) have the lowest priority, so the criterion for this kind of branching is examined as the last one. The details of above method can be found in [Ďurikovič, 1996].

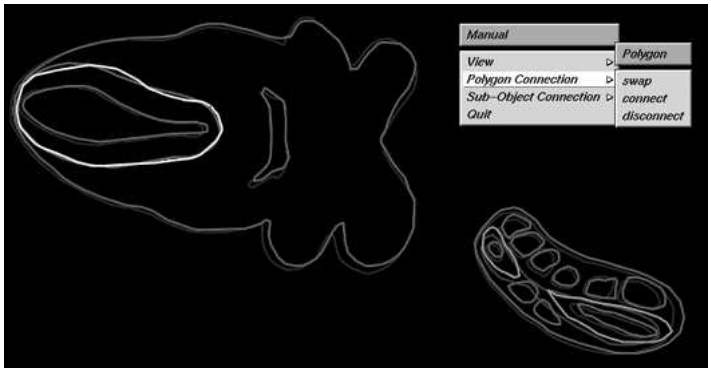

Fig. 2. Interface for the manual topology editor showing all contours of consecutive cross-sections drawn with different intensities for each section. The polygons creating a branch are colored green.

4.1 Topology Editor

The fully correct reconstruction from contours can not always be obtained because of many valid possibilities that are not acceptable. For example, employing automatic topology reconstruction in our data set correctly reconstructed 84% of all branches.

The remaining or erroneous branches had to be corrected manually. The corrections are controlled by the interactive selection of a pair of contours on the screen where all contours of two consecutive cross-sections are drawn (see Fig. 2).

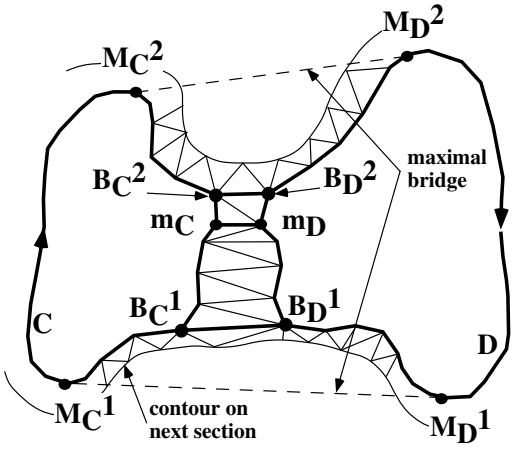

Fig. 3. Finding of bridge points on branch seen from above, $(\overline{B_C^2 B_D^2}; \overline{B_C^1 B_D^1})$ is automatically generated bridge.

5 Triangulation: Finding of Bridge Points

The space between two contours is filled by triangular patches generated automatically. Several methods referred as local [Christiansen and Sedeberg, 1987] and global [Fuchs et al., 1977] optimal methods are available. Often the local methods fail in some carefully design cases. The following is the proposed method [Ďurikovič, 1996] for triangulation of gap branches.

A gap branch can be reconstructed by horizontal triangular patches with two terminal segments, or *bridges*, specified automatically (see Fig. 3). Finding the bridge as a convex hull of the convex hulls of two contours [Choi and Park, 1994] is often inadequate because the area within the bridge is larger than is actually necessarily. First, the convex hull of two contours is found, and then the convex hull of those convex hulls is calculated. There are new segments $(\overline{M_C^2 M_D^2}; \overline{M_C^1 M_D^1})$ having end points in the different convex hulls of polygons. We call this solution the *maximal bridge*. The minimal segment between two contours determines the *minimal bridge*, segment $\overline{m_C, m_D}$. The "optimal" selection of the bridge lies somewhere between the minimal and maximal bridges.

Possible bridges are searched to find the one where the joint contour through the bridge segments is similar to the contour in the next section. The contours are considered similar [Gonzales and Wintz, 1987] when the factor $l^2/(4\pi A)$ has the most closer value for both contours. l and A are the perimeter and area, respectively, of the surrounded region. The candidates for bridge segments are all segments (X_C, Y_C) having $X_C \in [M_C^2 M_C^1]$ and $Y_C \in [M_D^1 M_D^2]$. To speed up the search of bridge segments we search only the set of segments generated by the Christiansen triangulation method within the maximal bridge segments $(\overline{M_C^2 M_D^2}; \overline{M_C^1 M_D^1})$. In order to avoid long segments, it is advantageous to establish a maximal limit for the length of the bridge segments relative to the minimal contour distance.

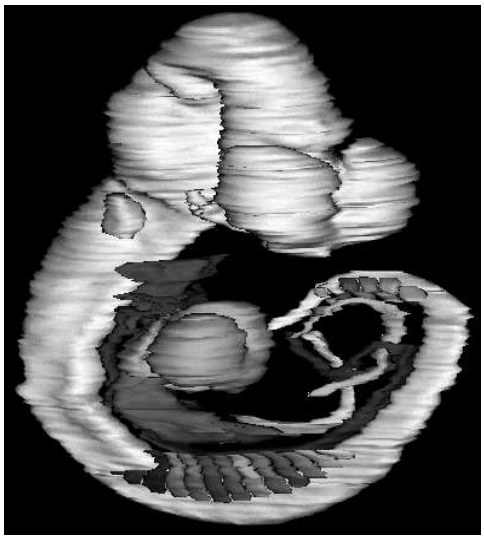

Fig. 4. Reconstructed topology of 54 objects of mouse embryo. Gray structure is a neural tube, light brown structure in the middle is a heart with blood vessels colored dark brown. Stomach is the structure behind the heart colored magenta.

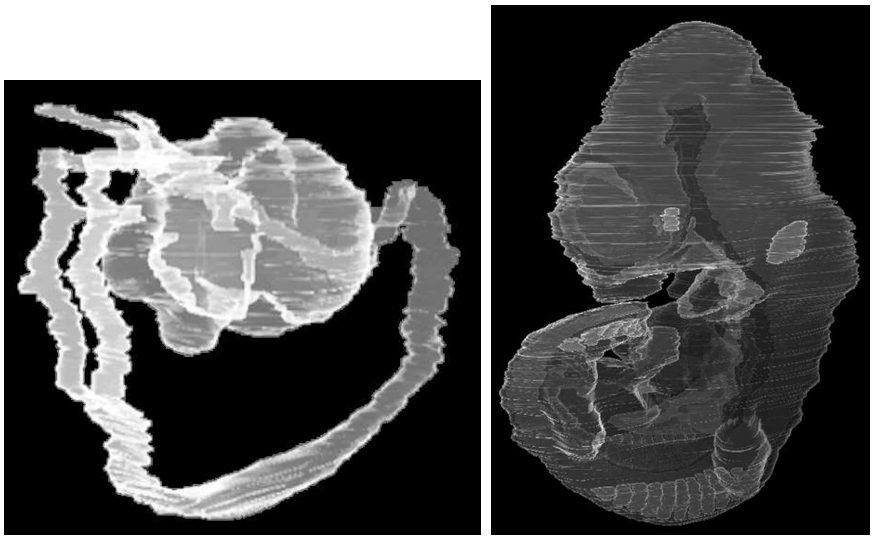

Fig. 5. Reconstructed mouse embryo. a) Transparent visualization of embryo's heart and blood vessels. b) Semi-transparent visualization of the entire mouse embryo.

6 Results

The proposed ACM was applied by the authors to the location of target organs within the microscopic images and to the 3D reconstruction of a mouse embryo. The new ACM offers a way to reduce the sensitivity of active contours to localized noise. The method is shown to be effective for refining estimates of an object's shape and location. Some organs consist of one or more branches. This phenomenon occurs within the series of cross-sections as the splitting of a contour when there is a different number of contours in two consecutive cross-sections. The result of automatical topology reconstruction is demonstrated in Fig. 4. This example contains several open and connected branches reconstructed correctly. Furthermore, when the triangular patches are generated, transparent and semi-transparent visualization techniques can be applied. The transparent visualization of the heart and blood vessels is shown in Fig. 5a. In Fig. 5b the entire mouse embryo is visualized. The proposed system is applied to data composed of 636 cross-sections and 54 structures of a mouse embryo.